

UM-HSRI-81-56

TRUCK TIRE TRACTION

Final Report  
Sub-Contract S8101

R.D. Ervin  
C.C. MacAdam

Highway Safety Research Institute  
The University of Michigan

December 1981



Technical Report Documentation Page

1. Report No.	2. Government Accession No.	3. Recipient's Catalog No.	
4. Title and Subtitle TRUCK TIRE TRACTION		5. Report Date December 1981	6. Performing Organization Code 019242
		8. Performing Organization Report No. UM-HSRI-81-56	
7. Author(s) R. Ervin and C. MacAdam		10. Work Unit No.	11. Contract or Grant No. Sub-Cont. S8101
9. Performing Organization Name and Address Highway Safety Research Institute The University of Michigan Huron Parkway and Baxter Road Ann Arbor, Michigan 48109		13. Type of Report and Period Covered Final 5-15-81/12-01-81	
		14. Sponsoring Agency Code	
12. Sponsoring Agency Name and Address Calspan Corporation* 4455 Genesee Street Buffalo, New York 14221		15. Supplementary Notes *Prime Contract No. DTNH-22-80-C-07093 National Highway Traffic Safety Administration U.S. Department of Transportation	
16. Abstract <p>The traction properties of heavy truck tires were measured using the HSRI Mobile Truck Tire Dynamometer on selected asphalt and concrete pavement sections at the Transportation Research Center of Ohio. A sample of eight test tires and five control tires were subjected to a sequence of longitudinal and lateral slip conditions on each of the two surfaces. Data were collected on analog magnetic tape during the field operations and later processed, in digital form, to produce condensed measures of traction behavior. The processed results are reported here without evaluation or discussion.</p>			
17. Key Words Truck Tires, Traction, Pavement Friction		18. Distribution Statement UNLIMITED	
19. Security Classif. (of this report) NONE	20. Security Classif. (of this page) NONE	21. No. of Pages 789	22. Price



## TABLE OF CONTENTS

1.	INTRODUCTION. . . . .	1
2.	METHODOLOGY . . . . .	2
2.1	Mobile Traction Measurement Apparatus. . . . .	2
2.2	Test Procedure . . . . .	11
2.3	Data Processing. . . . .	19
	APPENDIX A - Processed Results of Longitudinal Traction Tests. . . . .	30
	APPENDIX B - Processed Results from Lateral Traction Tests . . . . .	203



## 1.0 INTRODUCTION

This document constitutes the final report on an experimental project entitled "Truck Tire Traction" conducted by the Highway Safety Research Institute of The University of Michigan under Subcontract Number S8101 to the Calspan Corporation. The project entailed the conduct of truck tire traction measurements using an over-the-road dynamometer as part of a round-robin testing program being directed by Calspan under their prime contract, Number DTNH-22-80-C-07093, with the National Highway Traffic Safety Administration of the U.S. Department of Transportation.

Tests were conducted using the HSRI Mobile Truck Tire Dynamometer on selected asphalt and concrete pavement sections at the Transportation Research Center of Ohio. A sample of eight test tires were subjected to a sequence of longitudinal and lateral slip conditions on each of the two surfaces. In addition to the eight-tire sample, five test sequences were performed on control tires at periodic points in the program. Data were collected on analog magnetic tape during the field operations and later processed, in digital form, to produce condensed measures of traction behavior.

The report contains a description of the test device, in Section 2.1, and outlines the data collection and processing procedures in Sections 2.2 and 2.3, respectively. The processed longitudinal traction data are presented in Appendix A and the lateral traction data are presented in Appendix B.

## 2.0 METHODOLOGY

Traction tests were conducted during June and July, 1981, according to a set of test procedures which duplicated those performed during a previous NHTSA-sponsored study.\* The test program involved the exercise of longitudinal and lateral slip sequences on each of eight tire specimens, with five control tire tests being run in a pattern which meshed with the eight-tire sample. The test machine, the HSRI Mobile Truck Tire Dynamometer, was set up first in the configuration for making the longitudinal traction tests on the tire sample, and three weeks later, was operated in the lateral traction configuration for testing the sample. The test machine is described in Section 2.1 followed, in Section 2.2, by a description of the test procedure.

The data were collected in the field on FM analog tape and were later transcribed to digital format for processing. The data processing technique is described in Section 2.3.

### 2.1 Mobile Traction Measurement Apparatus

The HSRI mobile dynamometer in its current stage of development consists of a tractor-semitrailer vehicle which permits investigation of either longitudinal or lateral traction characteristics of heavy truck tires. The system permits measurement of longitudinal properties by way of the trailer-configured dynamometer as it is towed and serviced by the instrumented tractor. Mounted on the same tractor is a structure supporting a lateral traction measurement system, as diagrammed in the plan view of Figure 1. Each test system is basically designed to expose a truck tire specimen to a set of operating conditions which cover the full range of possible loads, velocities, longitudinal or angular slip, and pavements such as can be encountered under either normal or emergency situations on the highway.

The longitudinal traction dynamometer, shown in Figure 2, is a welded trailer structure of pipe and plate sections, designed for economy of construction and for stiffness. The test wheel is situated approximately at the trailer center-of-gravity position and is supported by a

---

\*P.L. Boyd, A.H. Neill, Jr., and J.A. Hinch, "Truck Tire Cornering and Braking Traction Study," Final Rept., Contract No. NHTSA-9-6227, Rept. No. DOT HS-804 732, March 1979.



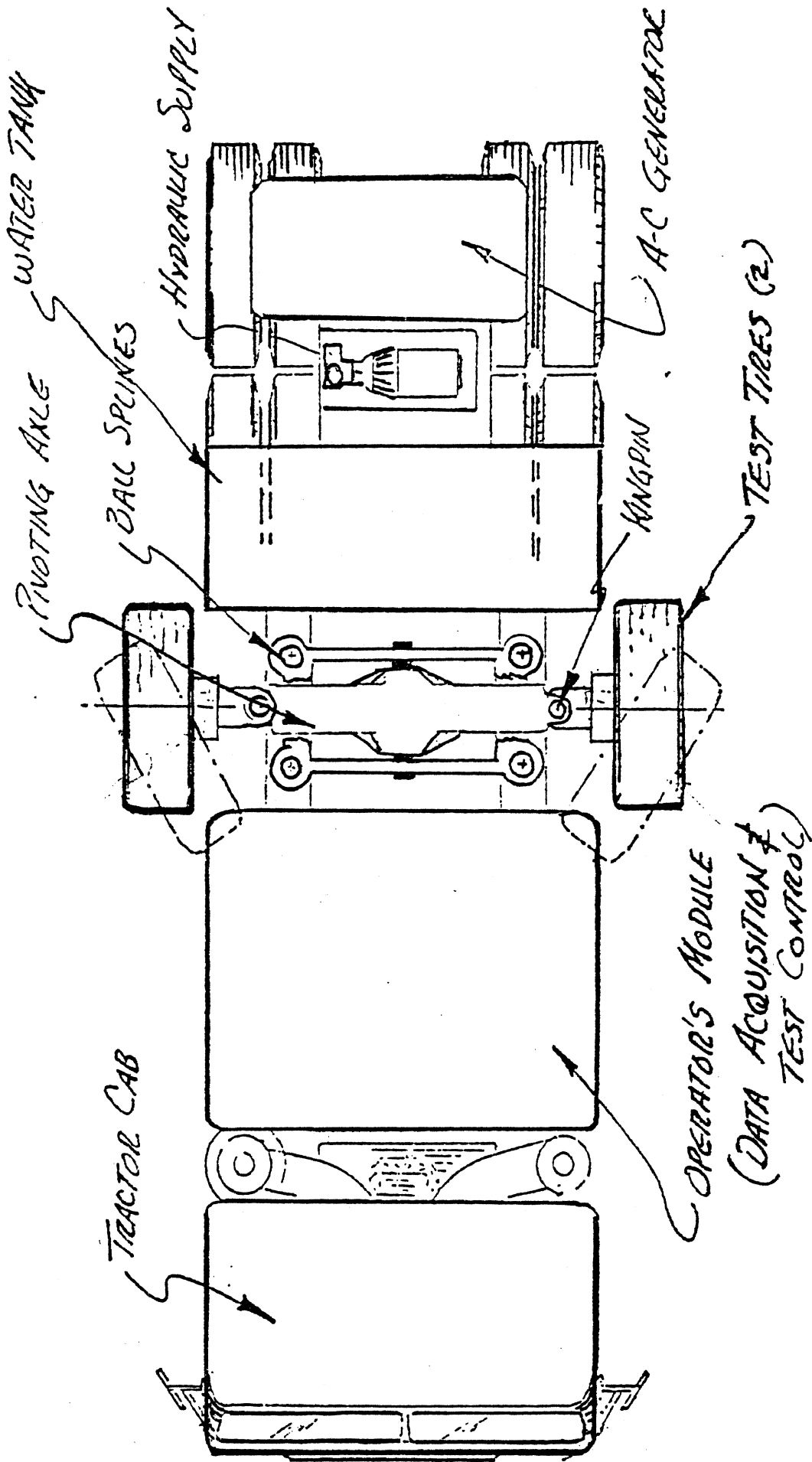


Figure 1. Plan view of Mobile Truck Tire Side Force Dynamometer.

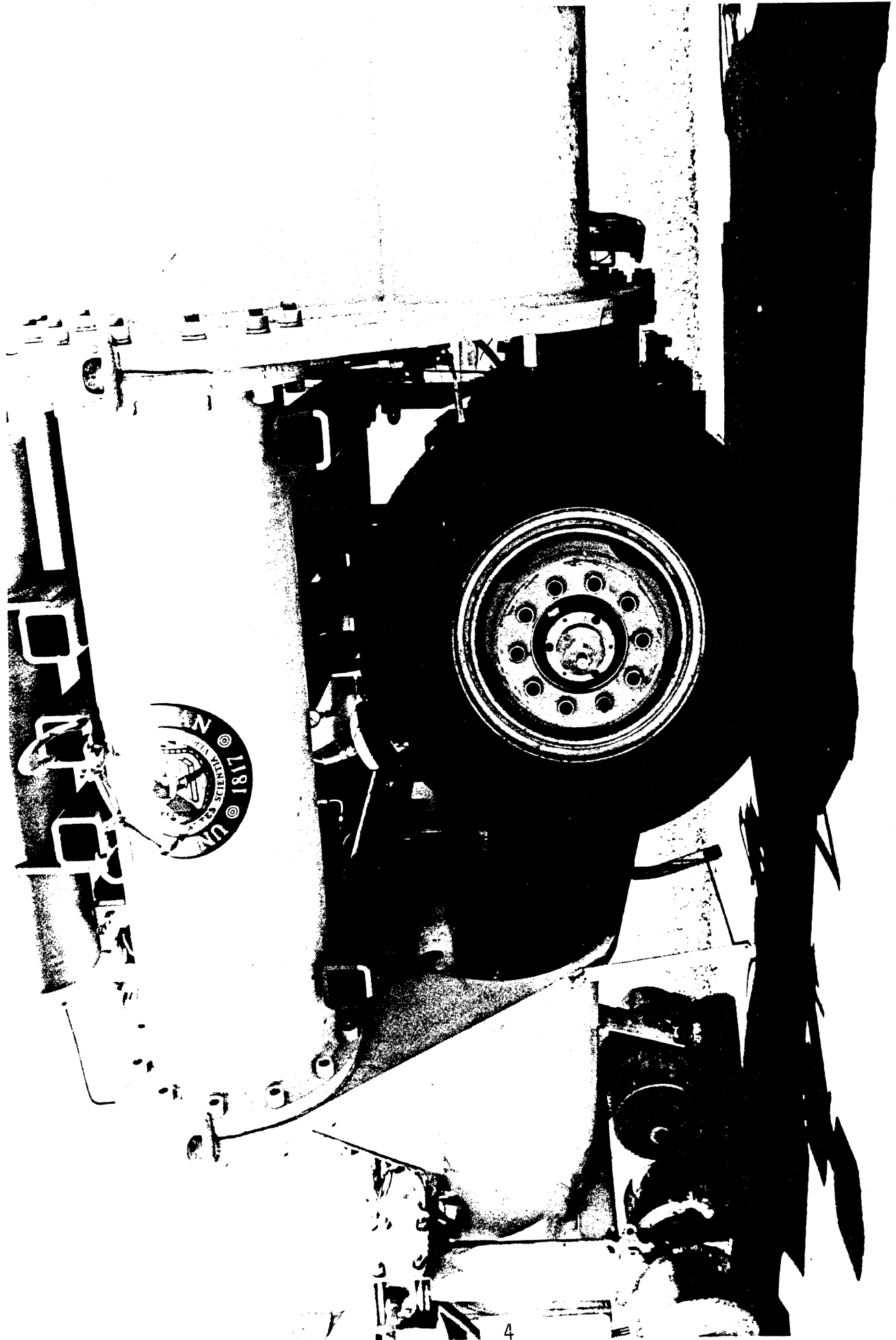


Figure 2. Test tire on longitudinal force trailer.

parallelogram suspension. This suspension configuration, shown in Figure 3, derives from attempts to achieve three fundamental qualities in a mobile traction measurement machine; namely,

- 1) the elimination of kinematic interactions between the loads applied to the test wheel and resulting shear forces and moments,
- 2) the employment of a low-spring rate loading mechanism (an air spring), to assure the attainment of the desired load levels while neither (a) sacrificing frequency response in the vertical degree of freedom of the test wheel, nor (b) imposing a significant through-coupling of the vibrations of the foundation vehicle to the test wheel, and
- 3) the minimization of the value of the "unsprung" mass, i.e., the mass which is displaced with the vertical motion of the test wheel spin axis.

The parallelogram linkage suspension is thus provided to assure kinematic isolation of forces while assuring a zero inclination (camber) of the test wheel plane.

The use of an air spring loading mechanism permits a controllable vertical load condition and, in the case of the HSRI machine, imposes a nominally 350 lb/in coupling between the trailer and the test wheel—while operating at a common mid-range load of 5000 lb,  $F_z$ . At higher loads, the spring rate rises to a maximum value of 1000 lb/in at a load of 20,000 lbs, while the spring rate, of course, diminishes to zero at zero inflation of the air spring. These spring rates contrast with corresponding leaf suspension rates of trucks which are five to thirty times stiffer at comparable rated wheel loads.

The basic design principle behind air spring loading, then, is that the machine incorporates a relatively "soft" loading member (which is also virtually frictionless) and thereby attains features which serve to enhance the quality of the vertical load condition which is imposed upon the test tire. With such a mechanism, it is then straightforward to

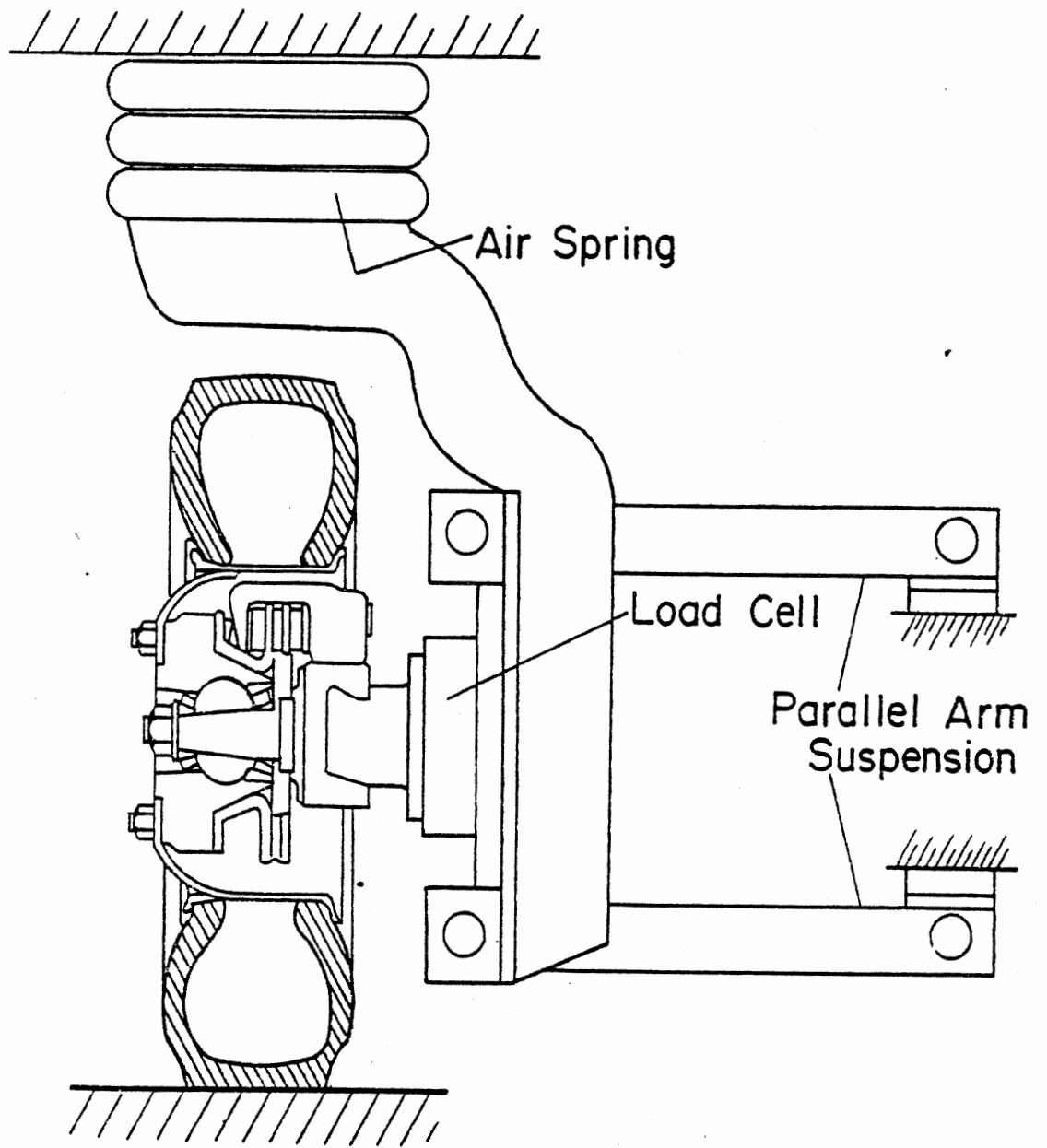


Figure 3. Test wheel suspension layout in the longitudinal traction measurement assembly.

obtain precision selections or vertical load through the use of commercially available precision regulators.

The unsprung mass which is associated with the vertical degree of freedom of the test wheel on the HSRI machine weighs 1850 lbs, when outfitted with a 10.00 x 20 load range F tire and the corresponding 20 x 7.50 disc wheel rim. By such a configuration, the "wheel hop" system indicates a natural frequency of approximately 5 Hz (for an effective radial spring rate of the tire of 5000 lb/in). In general, a high-frequency wheel hop system permits a minimal vertical load fluctuation as the tire follows the varying profile of the test surface. In the design of HSRI's longitudinal force dynamometer, the "quality" deriving from a reduced size of the unsprung mass was comprised with the obvious needs of strength, stiffness, and economy of construction of the wheel support assembly. The longitudinal force,  $F_x$ , vertical load,  $F_z$ , and brake torque,  $T_b$ , are transduced by way of a serial-mounted load cell. These signals, together with wheel angular velocity and vehicle velocity, constitute the primary data channels for the machine.

The nominal pitch and jounce trim of the HSRI trailer are controlled through the use of self-leveling air suspensions on both the trailer rear axle and the tractor rear tandem. Thus, as a given vertical load is transferred from the two respective axle sets to the test wheel, through inflation of the test wheel air spring, the tractor and trailer leveling systems adjust to a running equilibrium at which the trailer assumes its design trim attitude. The use of air suspensions on both ends of the trailer also contributes to attenuation of ride motions, thus further assuring quality in the vertical load condition.

The test trailer is capable of mounting any tire in the 20-inch rim size, and above, which is:

- a) less than 46 inches in free diameter, and
- b) 18 inches or less in maximum section width.

Tires can be loaded to a maximum level of 20,000 lbs, although, to date, brake torque limitations have prevented the lockup of tires on high friction surfaces at loads exceeding about 15,500 lbs.

The lateral traction dynamometer shown schematically in Figure 4 mounts two tire samples on opposing steerable spindles outboard of the tractor's wheel tracks. The two tires are "toed-in" together by an electrohydraulic servo system covering a slip angle range from  $-1^{\circ}$  to  $+30^{\circ}$ . The test wheel spindles are mounted upon a solid cross-axle which is constrained by a single longitudinal pivot pin.

The pin itself is fastened within a cage which can move only vertically, as constrained by a set of four ball-spline bearings. The vertically-"floating cage" is then loaded through inflation of a set of air springs. This machine thus incorporates a suspension designed to maximize the three "fundamental virtues" of mobile measurement described earlier—but for the more complicated case in which two tires are needed to achieve a side force equilibrium on the foundation vehicle. Clearly, the "pivot axle" arrangement provides for a load equalization between both tires while also providing a higher frequency response to road profile irregularities which are uncorrelated, side-to-side. The "floating cage" provides the needed kinematic isolation of the vertical load from forces in the ground plane by virtue of its rectilinear antifriction constraints. The air spring loading configuration again provides for precision load selection while incorporating a low spring rate coupling between the unsprung mass(es) and the foundation vehicle.

The two wheel spindles are "steered" to equal but opposing slip angles by an electrohydraulic servo system which incorporates two sets of actuating cylinders as shown in Figure 5. The linkage arrangement which mechanically couples both spindles together permits the use of a single control loop, operating on the feedback signal from the one instrumented wheel while assuring common slip angles, side-to-side, even in the event of a servo power failure.

The system permits mounting of any tire within the 30 to 48 inch range of free diameters and which is less than 18 inches in cross-section width. The measurement of tire force and moment conditions is achieved by way of a serial multicomponent load cell which transduces lateral and vertical force components as well as aligning moment.

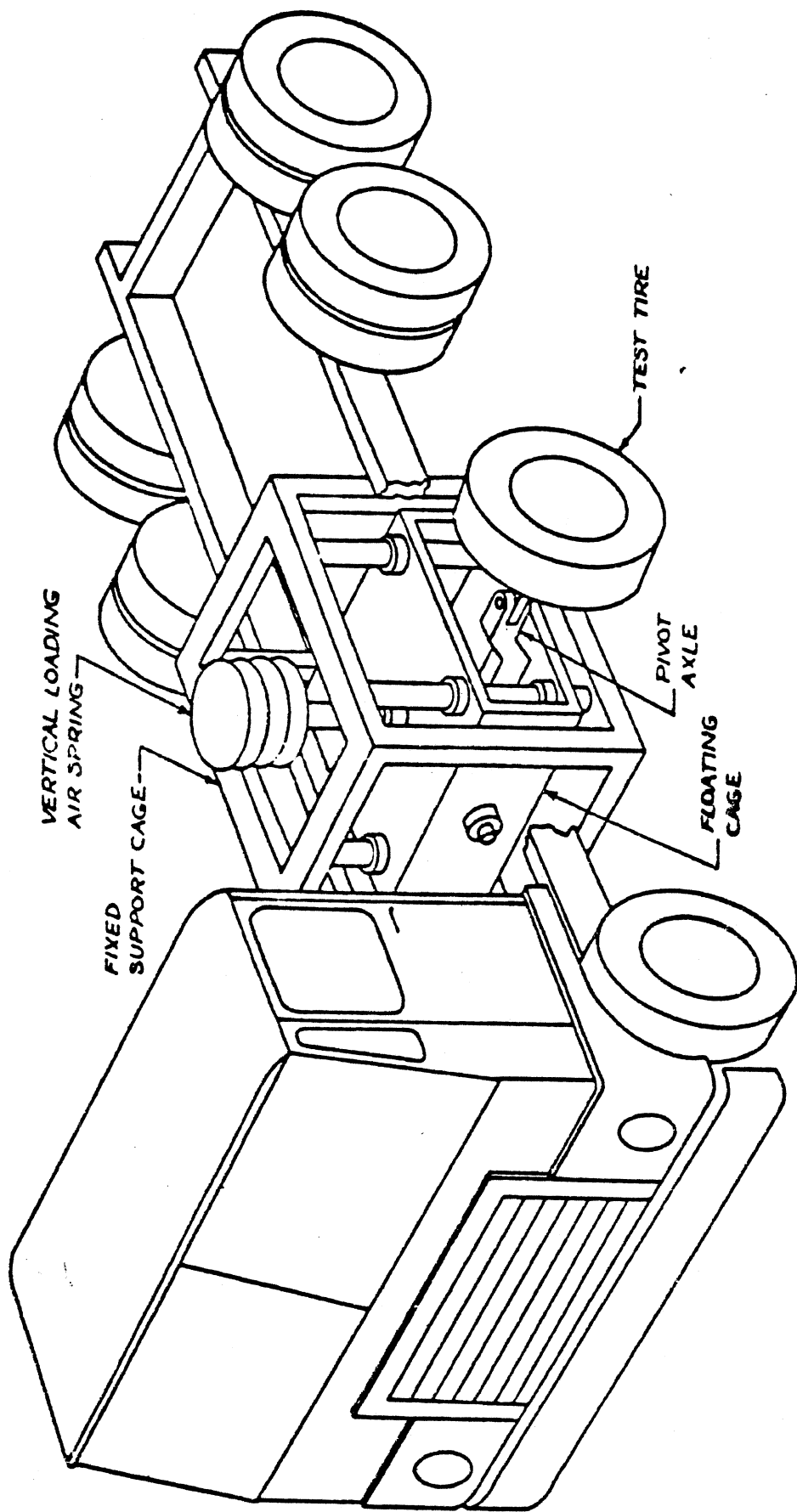


Figure 4. Major components of the side force dynamometer assembly.

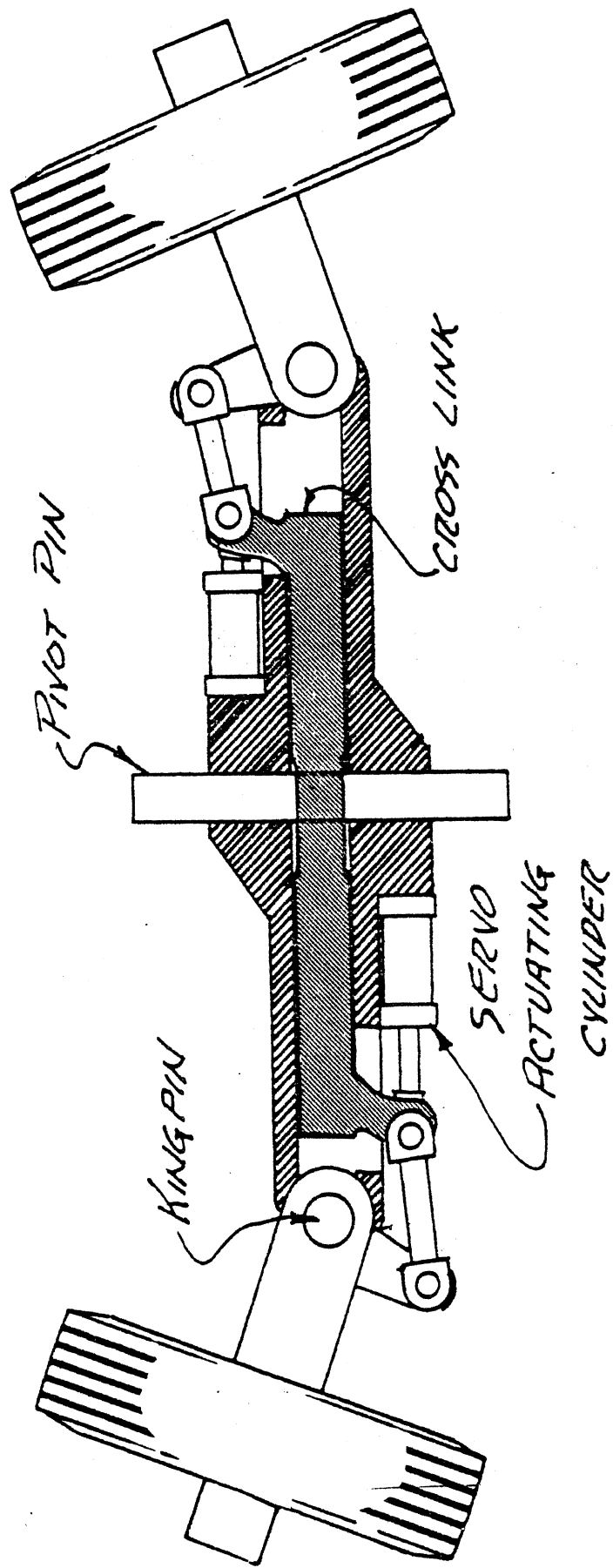


Figure 5. Section view of pivot axle with steering servo linkage.



Data signals from either the longitudinal or lateral test apparatuses are conditioned and recorded within a tractor-mounted module. The module serves as a self-contained data acquisition laboratory as well as the operator's station for selecting and initiating test control functions. As shown in Figure 6, the operator's module provides an array of hard-wired electrical controls in addition to certain pneumatic and hydraulic control elements.

## 2.2 Test Procedure

The mobile dynamometer exercised each tire in the longitudinal and lateral traction test series according to one basic matrix of conditions. The matrix included a single value of load, and the application of six sweeps of either longitudinal or lateral slip for each of two speeds and two surfaces. The overall test sequence required approximately 1-1/2 hours with each tire. In addition to traction measurements, certain test condition measurements were also made concurrently with the testing of each tire. The recorded data signals included the following:

$F_x$	longitudinal force
$F_y$	lateral force
$F_z$	vertical load
$V$	test vehicle velocity
$\omega$	wheel angular velocity
$\alpha$	slip angle

Data being recorded on FM magnetic tape were played back simultaneously and displayed to the test vehicle operator on a pen-chart recorder to provide for continuous assurance of nominal data quality. The traction measurements were made at the Transportation Research Center of Ohio. Shown in Figures 7a and 7b are diagrams of the Vehicle Dynamics Area at TRC, which provided an asphalt test surface, and the Skid Pad facility, which provided a polished concrete test surface. Tests were conducted on both surfaces using an on-board watering system for laying down an 18-inch-wide swath of water ahead of the test tire. The watering

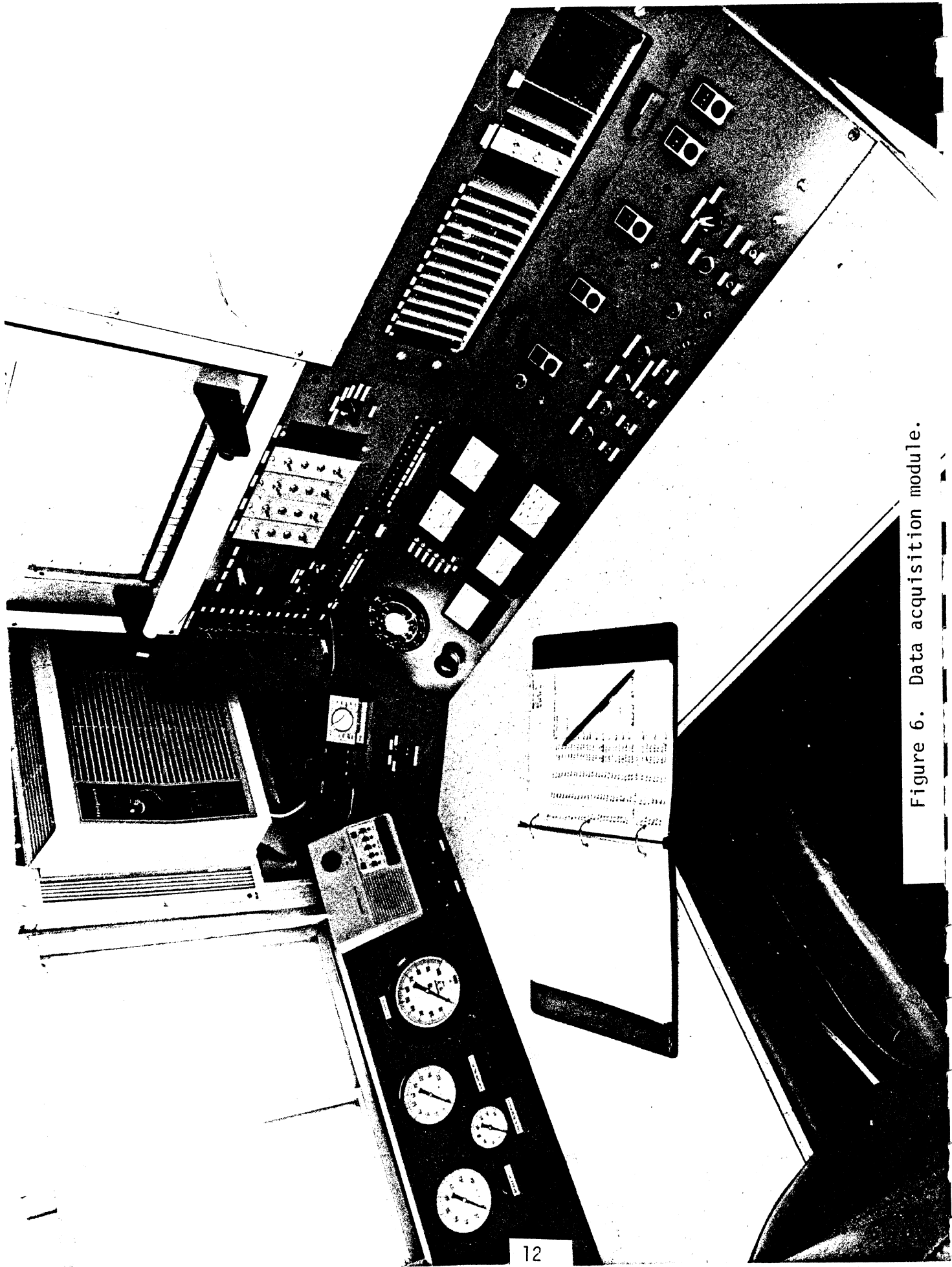


Figure 6. Data acquisition module.

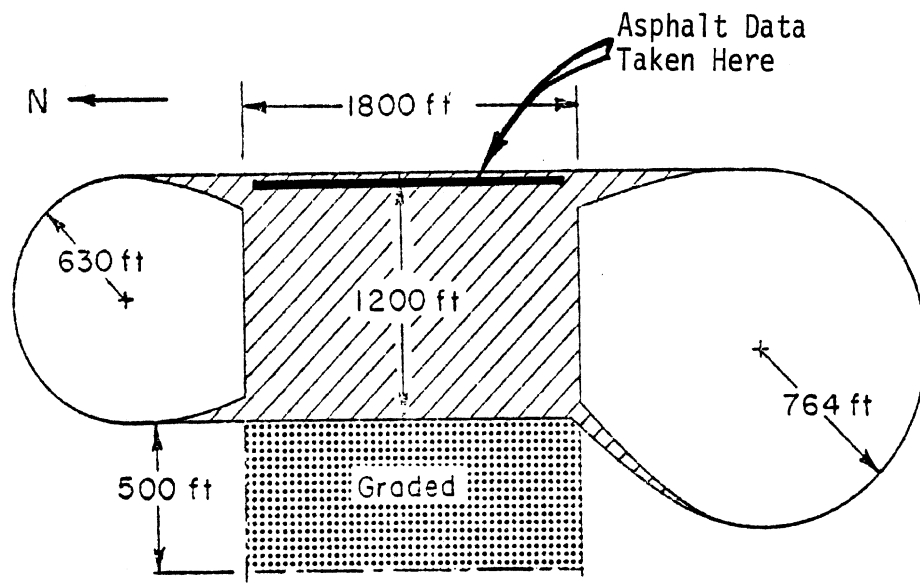


Figure 7a. Vehicle Dynamics Area at the Transportation Research Center of Ohio (TRC).

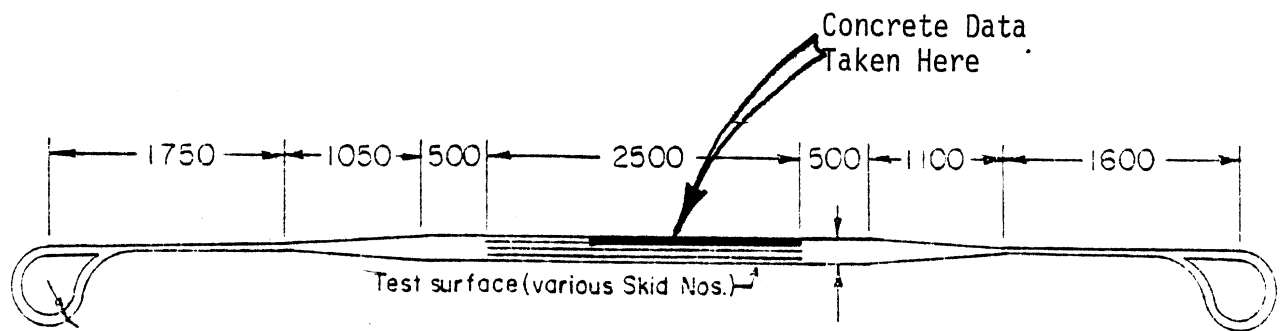


Figure 7b. Skid Pad at TRC.

system flow rate was adjusted in proportion to vehicle speed in order to establish a constant 0.020-inch nominal depth of the delivered water for the two test speeds, 40 and 50 mph. The following lists state the procedural steps by which were obtained the longitudinal and lateral traction measurements, respectively.

#### Longitudinal Traction Test Sequence

1. Initial measurement of the hardness of the tire's tread is made.
2. The tire is mounted on the test machine, loaded to 4,620 lbs, and is inflated (cold) to a pressure of 85 psi for bias tires and 90 psi for radial tires.
3. The machine is moved to the asphalt test track (VDA) with the tire raised and pretest calibration of instrumentation is performed. Measurements are made of the temperatures of the dry asphalt pavement surface and the temperature of the water in the on-board watering system tank. Weather conditions are logged, including ambient temperature, wind velocity and direction, and the general sky condition (sunny, overcast, etc.). The tire is lowered and loaded to 4,620 lbs.
4. Three warm-up laps\* ( $\approx 5.7$  miles) are performed on the asphalt track at a speed of 50-55 mph.
5. A pre-wet lap is made, delivering 0.020-inch depth of water at 40 mph and performing six brake applications (time to peak traction  $0.3 \text{ sec} \pm 0.1 \text{ sec}$ ) with the locked-wheel condition being sustained for 1 second and with a 1-second pause between the release of the brake at the end of one cycle and the reapplication of the brake at the initiation of the next.
6. Step 4 is repeated but test data are recorded throughout the braking sequences.
7. Step 6 is repeated, except at a speed of 50 mph.
8. The machine is stopped, the tire raised, and calibration of the instrumentation performed. The tire is inspected for damage.
9. The machine is moved to the polished concrete test track (skid pad), stopped, and the tire loaded to 4,620 lbs.

---

\*All tests on the asphalt track are made with the test machine moving in one direction (south).

10. The test lane of the concrete surface is pre-wetted, heading south, at 40 mph.
11. Three brake applications\* are made, heading north, at 40 mph delivering water and recording test data.
12. Step 11 is repeated (heading south).
13. Two brake applications are made, heading north, at 50 mph delivering water and recording data.
14. Step 13 is repeated (heading south).
15. Step 13 is repeated (heading north).
16. The machine is stopped, the tire raised, and a calibration of the instrumentation performed. The tire is inspected for damage. The temperature of the dry concrete surface is then measured.
17. A final measurement of the tread rubber hardness is performed after the tire has been dismounted and cooled to room temperature.

#### Lateral Traction Test Sequence

1. Initial measurement of the hardness of the tire's tread rubber is made.
2. The tire\*\* is mounted on the test machine, loaded to 4,620 lbs and its cold inflation pressure set to 85 psi for bias tires and 90 psi for radial tires.
3. The machine is moved to the asphalt test track (VDA) with the tire raised and a pretest calibration of instrumentation is performed. Measurements are made of the temperatures of the dry asphalt pavement surface and the temperature of the water in the on-board watering system tank. Weather conditions are logged, including ambient temperature, wind velocity and direction, and the general sky condition (sunny, overcast, etc.). The tire is lowered and loaded to 4,620 lbs.
4. Three warm-up laps are performed (~5.7 miles) on the asphalt track at a speed of 50-55 mph.

---

\*More than one pass over the concrete surface is needed in order to fit the traction test cycles onto the available length of this low-friction surface. At 40 mph, three lockup cycles are conducted with each pass. At 50 mph, two lockup cycles are conducted per pass.

\*\*A "dummy" tire must be installed in a complementary position to balance side forces on the test machine.

5. A pre-wet lap\* is made, delivering 0.020-inch depth of water at 40 mph and performing the following linear slip-angle sweeps at a rate of 8 deg/sec: 0° to 20° to 0° to 20° to 0° (new tire only).
6. A data-recording run is made on the next lap while executing the slip angle sequence\*\* shown in Figure 8a.
7. Step 6 is repeated, except at a speed of 50 mph.
8. The machine is stopped, the tire raised, and a calibration of the instrumentation performed. The tire is inspected for damage.
9. The machine is moved to the polished concrete test track (skid pad), stopped, and the tire lowered and loaded to 4,620 lbs.
10. The test lane of the concrete surface is pre-wetted, heading south, at 40 mph.
11. A data-recording run is made on the next lap, heading north, while executing the slip angle sequence shown in Figure 8b at 40 mph.
12. Step 11 is repeated (heading south).
13. Step 11 is repeated (heading north).
14. A data-recording run is made on the next lap, heading south, while executing the slip angle sequence shown in Figure 8c at 50 mph.
15. Step 14 is repeated (heading north).
16. Step 14 is repeated (heading south).
17. The vehicle is stopped, the tire lifted, and a calibration of the instrumentation performed. The tire is inspected for damage. The temperature of the dry concrete surface is measured.
18. A final measurement of the tread rubber hardness is performed after the tire has been dismounted and cooled to room temperature.

---

\*All tests on the asphalt track are made with the test machine moving in one direction (south).

\*\*The slip angle sequence is selected to provide six "legs" of swept slip angle—three upgoing and three downgoing. On the asphalt surface, the six "legs" are achieved in a continuous, three-cycle, triangular waveform. On the concrete surface, the six "legs" are achieved by means of individual (two-leg) triangles.

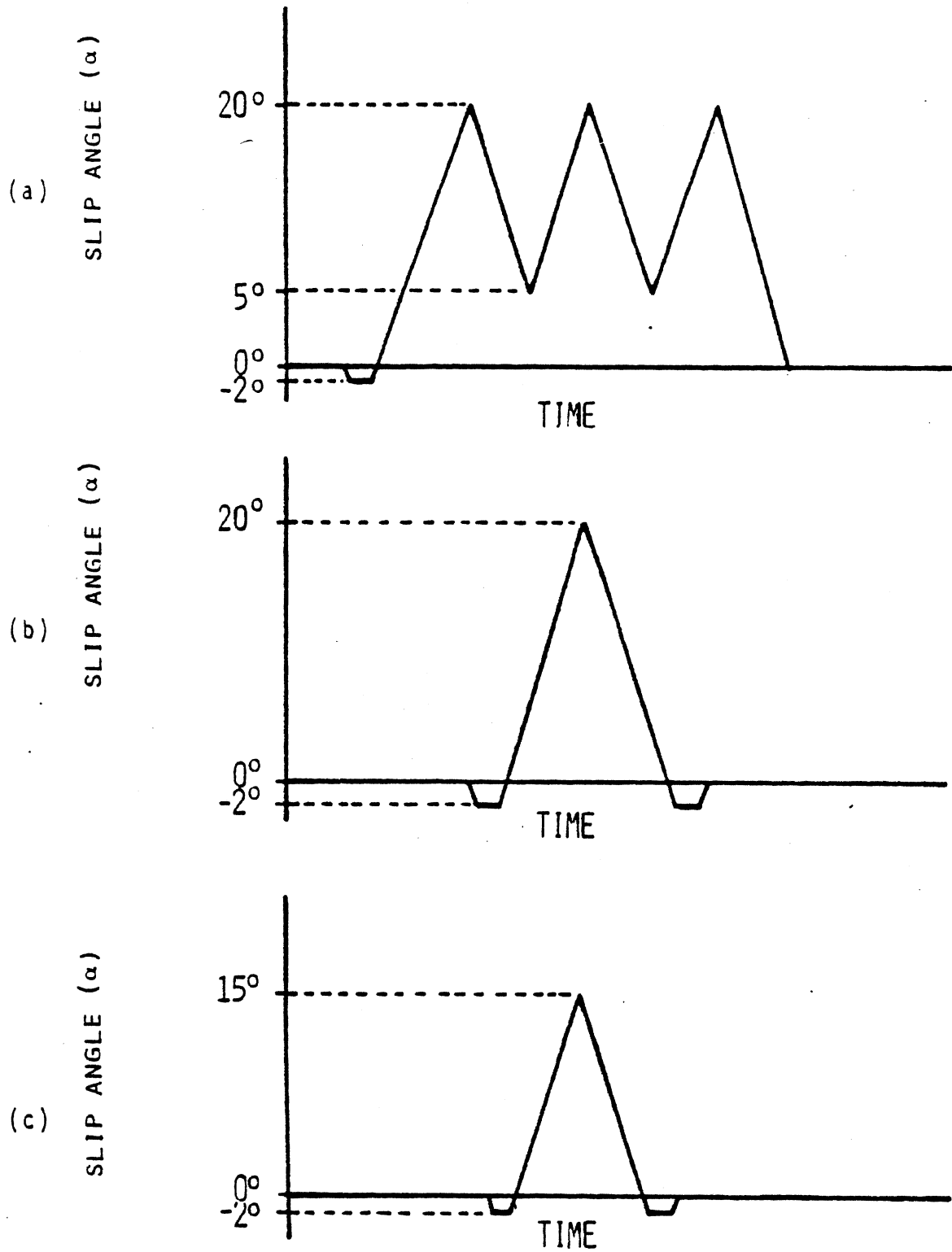


Figure 8. SLIP ANGLE TEST SEQUENCE FOR TESTS ON:  
 (a) Asphalt Surface @ 40 & 50 MPH  
 (b) Concrete Surface @ 40 MPH  
 (c) Concrete Surface @ 50 MPH

In addition to traction measurements on truck tires, measurements of the ASTM skid number were also made by TRC on the asphalt and concrete surfaces before and after the test program.

The longitudinal and lateral test procedures were conducted over a 13-tire sequence. Listed in Table 1 are the sequences in which each of the coded tires was tested. The code letters indicate the following:

"C" represents a control tire

"RR and RL" represent Radial-ply carcass constructions with Rib-type and Lug-type tread patterns, respectively

"BR and BL" represent Bias-ply carcass constructions with Rib-type and Lug-type tread patterns, respectively

Table 1. Sequence in Which Tire Samples Were Tested.

Order	Tire Code Nos.:	Longitudinal Series		Lateral Series	
		Control Tires	Test Tires	Control Tires	Test Tires
1		C1		C9	
2			BR-1		BR-1
3			RR-1		RR-1
4		C2		C2	
5			BL-1		RL-1
6			RL-1		BL-1
7		C2		C9	
8			BR-2		RR-6
9			RR-2		BR-6
10		C1		C2	
11			BL-2		RL-6
12			RL-2		BL-6
13		C1		C9	



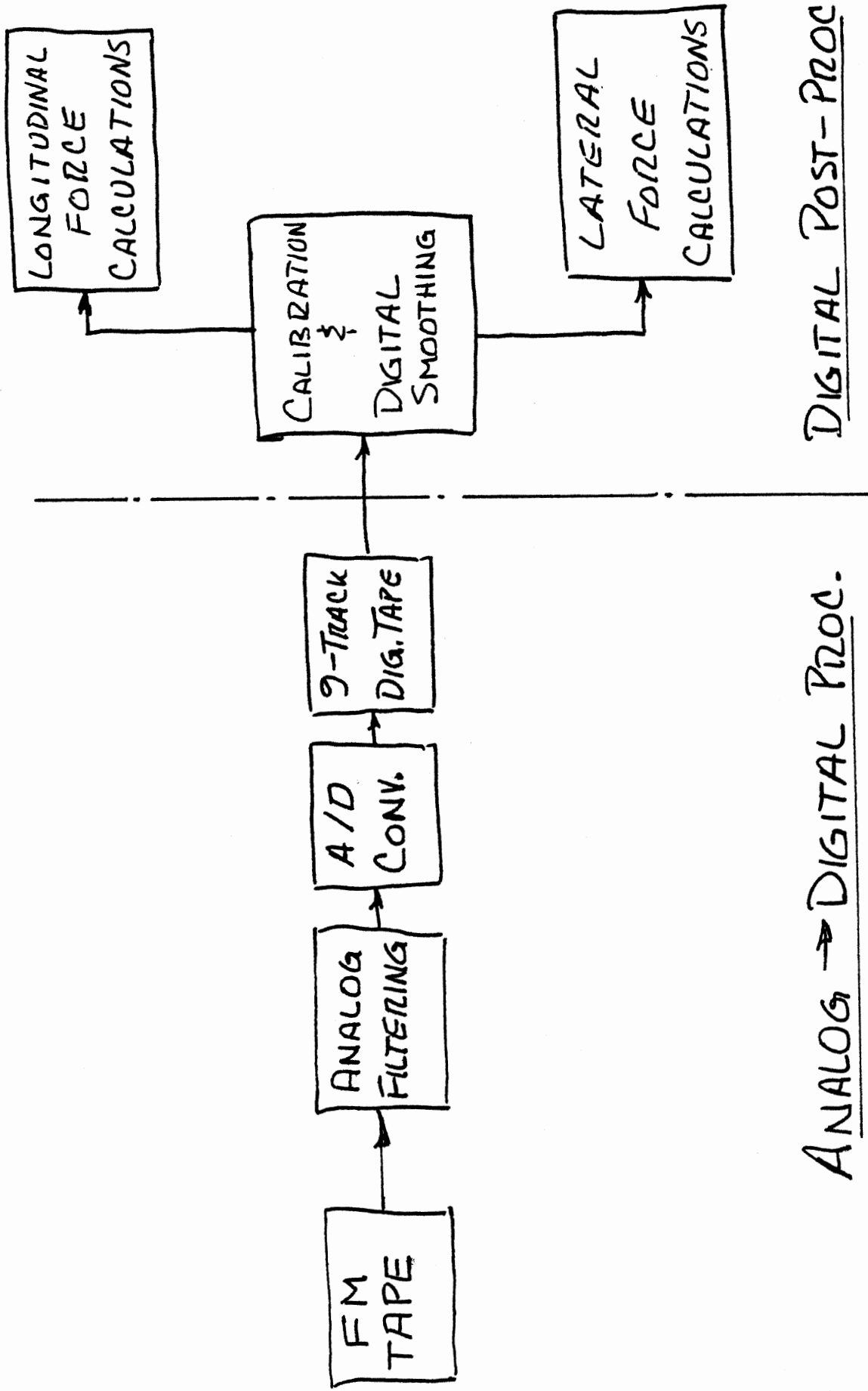
## 2.3 Data Processing

The block diagram shown in Figure 9 describes the different stages of data processing for both the longitudinal and lateral traction measurements. The initial steps in both processing sequences are nearly identical, differing only in the amount of analog filtering used and the rate at which data was digitized. The principal differences between lateral and longitudinal data processing occur following the analog-digital conversion, during the digital, "post-processing" calculations.

2.3.1 Longitudinal Tire Force Data Processing. The longitudinal tire force data were filtered at 10 Hz through single-pole filters and digitized at approximately 150 Hz. The variables digitized included longitudinal force ( $F_x$ ), vertical load ( $F_z$ ), brake torque ( $T_b$ ), rotational velocity ( $\omega$ ), and wheel translational velocity ( $V$ ).

The digital processing involved (a) calibration of each channel based on the zero, full-scale, and zero data signal levels which are recorded before and after each tire test sequence and based on the known load cell cross-talk sensitivities; (b) digital smoothing of each channel by a simple seven-point moving average calculation; (c) local least-squares curve fitting of each normalized traction ( $F_x/F_z$ ) versus longitudinal slip data set in order to obtain normalized traction data at specific values of longitudinal slip for subsequent averaging; and (d) final averaging of all valid test repeats, at each slip level along the way toward lockup, for each loading/velocity condition in the test series.

The least-squares curve-fitting procedure referred to above involves performing a linear least-squares regression for four digitized pairs of ( $F_x/F_z|_i$  vs slip $|_i$ ) and calculating new data pairs of ( $F_x/F_z|_k$  vs slip $|_k$ ) at specified values of slip $|_k$  from the regression. This regression procedure is repeated for the entire range of data from 0 slip to 1.0, shifting by one point each time it is performed. The specific values of slip $|_k$  were in increments of 0.02 from 0 to 0.20 and in 0.05 increments from 0.20 to 1.0.



ANALOG → DIGITAL PROC.

DIGITAL POST-PROC.

Figure 9. Tire force data processing.

A final average table was produced from a simple average of all the individual  $F_x/F_z|_k$  vs slip $|_k$  tables. Each final average table appears in a printout of the form shown in Figure 10, with a tabulation of SLIP and MUX ( $\underline{\Delta} F_x/F_z|_k$ ). Brake torque (TORQUE) and longitudinal tire force (FX) also are shown in Figure 10. The summary numerics appearing on the right-hand side of Figure 10 are defined as follows:

TQAV is the average brake torque at wheel lock ( $= \bar{F}_x \cdot \text{Loaded Radius}$ ) in lbs.

LOAD is the average vertical load prevailing just prior to a brake application, lbs.

VEL is the nominal velocity at which the test sequence was conducted, mph.

MUPEAK is the peak value of  $F_x/F_z|_k$  from the final average table.

MULOCK is the locked-wheel value of  $F_x/F_z|_k$  from the final average table.

RATIO is the ratio of MUPEAK to MULOCK.

Figure 11 shows the next page included in the printout which contains a plot of MUX VS SLIP. The above numerics are duplicated at the bottom of this page for convenience.

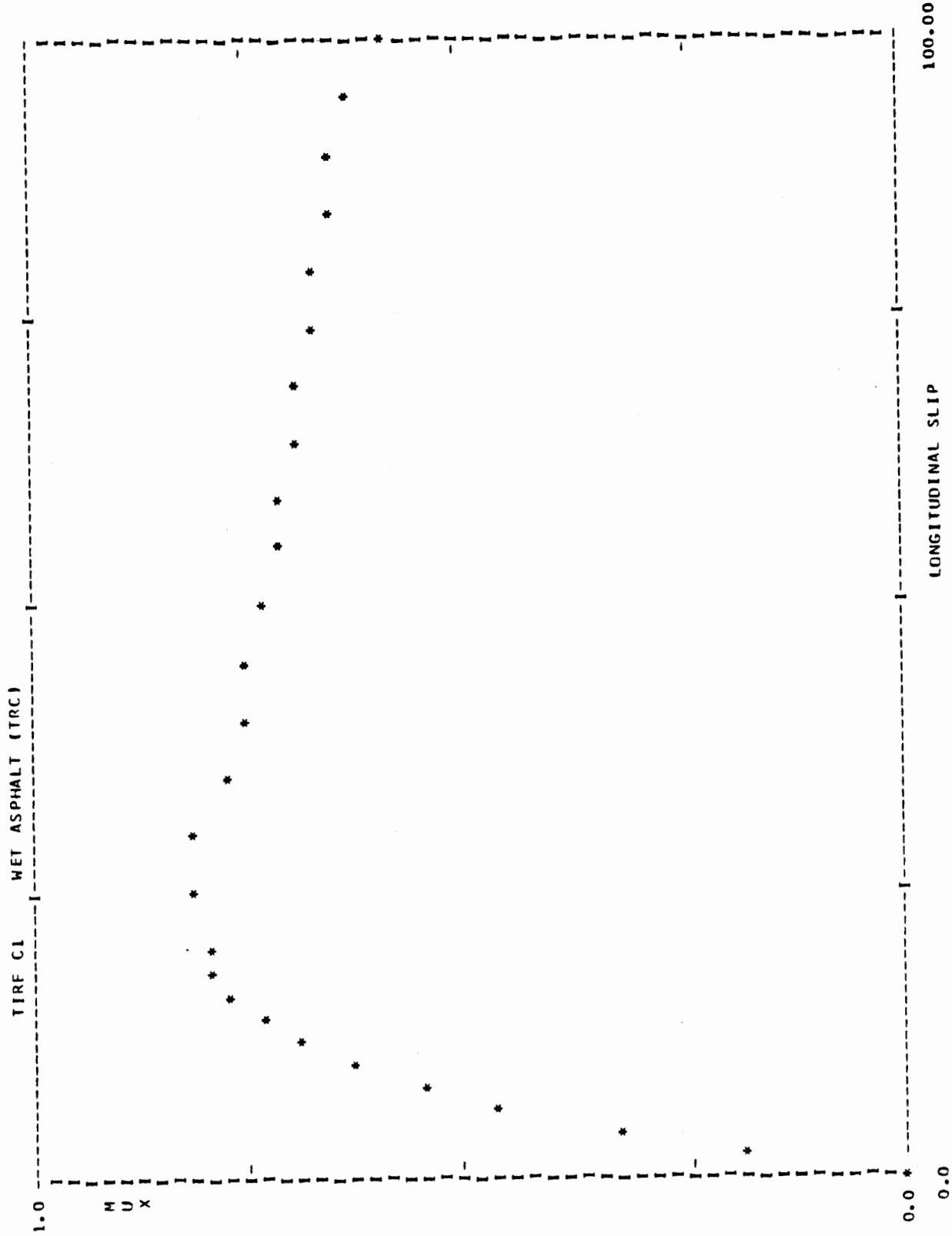
Figure 12 is an additional page from the printout showing values of  $F_x/F_z|_k$  from each of the individual lockup cycles at the cited test conditions, along with the value of slip at which each peak occurred. These values are shown in the Figure 12 printout as MU-PEAK, SLIP@PEAK, and MU-LOCK. Average values and standard deviations for the individual MU-PEAK and MU-LOCK values are shown as the last two items on the Figure 12 listing.

\*\* A-D FILE 4 NEW FILE 1 TEST SAMPLE101 \*\*  
 AVERAGE OF FILE 4 FOR 6 RECORDS. TIRE C1 WET ASPHALT (TRC)

SLIP	MUX	TORQUE	FX
0.0	0.00	0.0	0.0
0.02	0.18	17234.6	824.1
0.04	0.33	31689.8	1501.2
0.06	0.46	44608.5	2101.7
0.08	0.56	53717.7	2540.7
0.10	0.64	61685.2	2928.5
0.12	0.69	66962.0	3177.8
0.14	0.73	71218.4	3334.9
0.16	0.77	74371.2	3468.4
0.18	0.79	77488.5	3599.8
0.20	0.81	80002.0	3677.2
0.25	0.83	83781.1	3751.4
0.30	0.81	86109.9	3717.6
0.35	0.79	87595.6	3606.6
0.40	0.77	88869.8	3498.3
0.45	0.75	89882.9	3401.7
0.50	0.73	90735.7	3315.5
0.55	0.72	91590.9	3245.7
0.60	0.71	92394.2	3179.7
0.65	0.70	92695.3	3120.8
0.70	0.69	91759.1	3068.2
0.75	0.68	88461.8	3020.5
0.80	0.67	82093.6	2975.7
0.85	0.66	75686.7	2926.5
0.90	0.65	69772.4	2864.2
0.95	0.64	63954.6	2812.6
1.00	0.60	55958.3	2707.0

TQAV = 55958.3 LOAD = 4622.8 VEL = 40.0 MPH.  
 MUPEAK = 0.83 MULOCK = 0.60 RATIO = 1.37

Figure 10. Sample printer tabulated output--longitudinal force average table.



FZ = 4622.8 VEL = 40.0 MULOCK = 0.60 MUPEAK = 0.83 RATIO = 1.37 A-D FILE 4 NWFIL 1 SAMPLE 101

Figure 11. Sample page printer plot of normalized longitudinal force data.

MU-PEAK	SLIP&PEAK	MU-LOCK
0.893	0.250	0.597
0.831	0.250	0.613
0.770	0.200	0.592
0.869	0.250	0.623
0.774	0.200	0.597
0.804	0.250	0.562

MU-PEAK AVERAGE VALUE AND STD. DEVIATION : 0.824 0.050

MU-LOCK AVERAGE VALUE AND STD. DEVIATION : 0.597 0.021

Figure 12. Sample printer output - normalized longitudinal force - individual peak and slide values.

2.3.2 Lateral Tire Force Data Processing. Lateral tire force data were filtered at 10 Hz through three-pole filters and digitized at 50 Hz. Four variables were digitized; namely, lateral force ( $F_y$ ), vertical load ( $F_z$ ), slip angle ( $\alpha$ ), and forward velocity ( $V$ ).

As in the case of the longitudinal force data, the digital processing scheme involved (a) calibration of each channel based on the zero, full-scale, and zero data signal levels which were recorded before and after each tire test sequence and on the linear load cell cross-talk sensitivities; (b) digital smoothing of each channel by a simple nine-point moving average; (c) construction of individual normalized traction ( $F_y/F_z$ ) versus slip angle ( $\alpha$ ) tables for each positive-going and negative-going "leg" of the triangular slip angle waveform; and (d) averaging of the individual ( $F_y/F_z$ ) versus  $\alpha$  tables into one final average table. The individual and average tables used a one-degree increment in slip angle to describe the ( $F_y/F_z$ ) versus  $\alpha$  characteristic.

The printed output from the lateral force processing includes (a) individual tables of  $F_y/F_z$  versus  $\alpha$  (one for each "leg" of the triangular waveform of  $\alpha$ ), (b) the corresponding average table, and (c) a print-plot of the average  $F_y/F_z$  versus  $\alpha$  data.

Figure 13 shows a sample printout of an individual table. The labels ALPHA, FY, FZ, and MUJ correspond to slip angle ( $\alpha$ ), lateral tire force ( $F_y$ ), vertical load ( $F_z$ ), and the normalized traction coefficient ( $F_y/F_z$ ), respectively. Figure 14 shows a sample printout of an average table. The same column heading definitions apply to this table, with the additional numerics defined as follows:

AVE. LOAD is the average vertical load prevailing just prior to the initial slip angle application.

PEAK MUJ is the peak value of  $(F_y/F_z) = MUJ$  occurring in the average table.

@ALPHA is the slip angle value corresponding to the PEAK MUJ value.

ALPHA	FY	FZ	MUY
0.0	0.0	0.0	0.0
0.0	0.0	0.0	0.0
0.9	575.5	4620.5	0.125
2.0	1046.4	4713.5	0.222
2.9	1339.3	4560.8	0.294
4.0	1695.4	4661.6	0.364
5.0	1907.8	4451.6	0.429
5.9	2183.5	4638.8	0.471
7.1	2384.5	4649.7	0.513
8.1	2528.1	4724.8	0.535
9.0	2528.1	4575.4	0.553
10.0	2614.2	4507.8	0.580
10.9	2717.6	4583.1	0.593
12.1	2832.4	4604.1	0.615
13.0	2820.9	4572.1	0.617
13.9	2775.0	4455.7	0.623
14.9	2775.0	4426.9	0.627
15.9	2987.5	4699.7	0.636
17.0	2941.5	4577.5	0.643
18.1	2901.3	4600.6	0.631
19.0	2683.1	4349.2	0.617
20.0	2740.5	4491.9	0.610

BLOCK 53

Figure 13. Sample printer output--lateral force individual table.



TIRE C9 WET ASPHALT 40 MPH RUN O1  
 AVERAGE TABLE: ALPHA MUY FY FZ AVE. LOAD : 4563. PEAK MUY : 0.649 @ ALPHA : 17.0

ALPHA	MUY	FY	FZ
-0.7	-0.042	-194.0	4655.6
0.0	0.013	58.7	4548.9
1.0	0.116	546.8	4727.3
2.0	0.205	974.7	4759.3
3.0	0.290	1350.8	4656.0
4.0	0.364	1695.4	4661.6
5.0	0.427	1979.6	4635.7
6.0	0.476	2168.2	4557.9
7.0	0.513	2337.6	4559.8
8.0	0.541	2502.2	4622.7
9.0	0.567	2596.0	4576.4
9.9	0.592	2663.0	4495.8
11.0	0.613	2735.8	4463.7
12.0	0.626	2810.4	4486.8
13.0	0.638	2896.6	4540.8
14.0	0.644	2916.7	4526.4
15.0	0.646	2865.9	4435.4
16.0	0.649	2918.6	4499.2
17.0	0.649	2925.3	4507.8
18.0	0.646	2909.0	4499.3
19.0	0.643	2890.8	4492.3
20.0	0.642	2871.7	4472.5

AVE. PEAK MUY : 0.660      STD. DEV. : 0.029

Figure 14. Sample printer tabulated output--lateral force average table.

AVE. PEAK MUY is the average of the peak values of  $(F_y/F_z)$  shown on the individual  $(F_y/F_z)$  versus  $\alpha$  tables.

STD. DEV. is the standard deviation of the AVE. PEAK MUY value.

Finally, Figure 15 shows the corresponding print-plot for  $F_y/F_z$  versus  $\alpha$  from the average table.

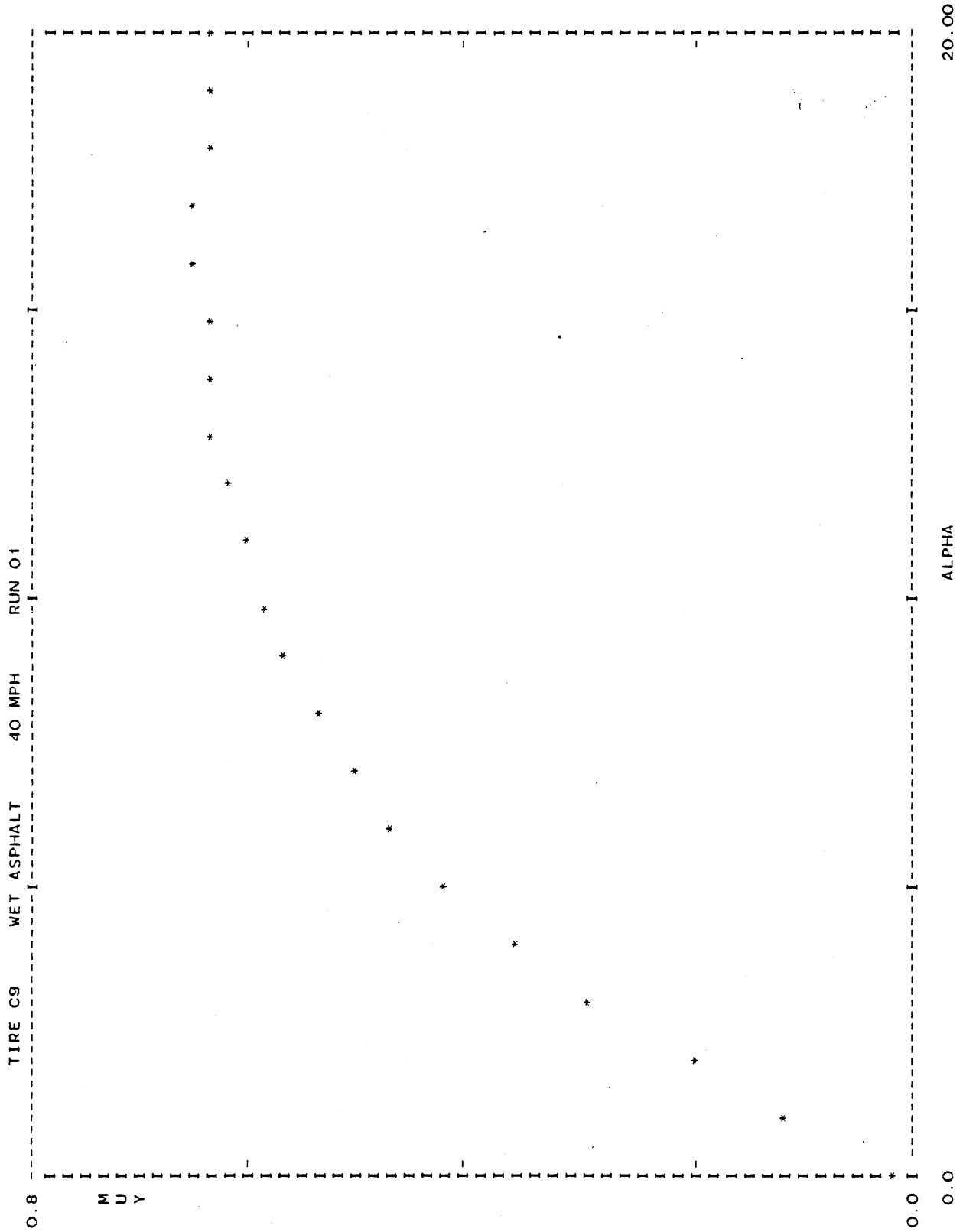


Figure 15. Sample page printer plot of normalized lateral force data.

